Reverse transcriptase inhibitors induce autophagy in a LINE-1 ORF1p-dependent manner

Michela Damizia[1,8,§], Mirko Baranzini[1,9,§], Ilaria Sciamanna[2,11], Ludovica Altieri[1], Paola Rovella[1], Omar G. Rosas Bringa[3], Samira Hozeifi[3], Leila J Saba[3], Apostolos Mourtzinos[3], Anna O'Shea[3], Mohammad Salik Zeya Ansari[1,11], Federica Andreola[4], Roberto Cirilli[2], Gianluca Sbardella[5], Annalucia Serafino[4,12], Gerald G. Schumann[6], Daniela Trisciuoglio[1], John LaCava[3,7,13], Patrizia Lavia[1], Corrado Spadafora[4]

[1] Institute of Molecular Biology and Pathology (IBPM), CNR Consiglio Nazionale delle Ricerche, c/o Department of Biology and Biotechnology, Sapienza University of Rome, 00185, Rome, Italy

[2] ISS Istituto Superiore di Sanità, 00161, Rome, Italy

[3] European Research Institute for the Biology of Ageing, University Medical Center Groningen, Groningen, The Netherlands

[4] Institute of Translational Pharmacology (IFT), CNR Consiglio Nazionale delle Ricerche, 00133, Rome, Italy

[5]Department of Pharmacy, University of Salerno, 84084 Fisciano, SA, Italy

[6] Division of Hematology, Cell- and Gene Therapy, Paul-Ehrlich-Institute, Langen, Germany

[7] Laboratory of Cellular and Structural Biology, The Rockefeller University, New York, NY, USA

[8] present address CIBIO Department of Cellular, Computational and Integrative Biology, University of Trento, 38123 Trento, Italy

[9] present address NIH National Institute on Aging, Baltimore MD 21224, USA

[10] present address Department of Neuroscience, Section of Human Anatomy, Catholic University of the Sacred Heart, 00168 Rome, Italy

[11,12]corresponding authors: ilaria.sciamanna@iss.it, annalucia.serafino@cnr.it,

[13] correspondence for mass spectrometry-based proteomics jlacava@rockefeller.edu

§ These authors contributed equally

Supplementary material

Contents

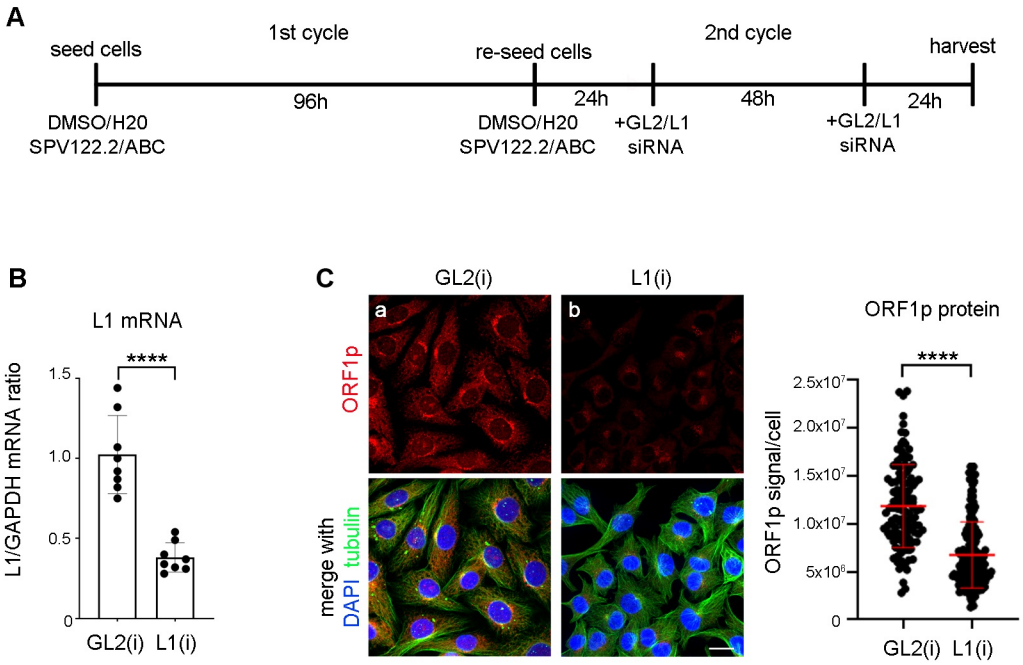

Supplementary Figure 1

Supplementary Fig. 1. Validation of L1(i)-mediated interference with *LINE-1* (henceforth *L1*) expression. A. Schematics of the *L1* interference approach. The regions of *L1* mRNA complementary to the L1-specific siRNAs s552967, s552968 and s552969 (all three together are designated as L1(i) and drawn as red bars) are indicated in Fig. 1A. **B.** Validation of the efficiency of L1(i) siRNAs by RT-PCR: L1-specific mRNA levels were significantly down-regulated after transfection with L1(i) siRNAs compared to luciferase-specific (GL2(i), control) siRNAs in PC3 cells. Histograms represent the relative expression of *L1* mRNA in control (GL2, set as 1) and L1(i)-transfected cells after normalization to GAPDH transcript levels. Ratios were calculated using the 2-ΔΔCT method. Data are presented as the mean ± SD from eight independent experiments. The statistical significance was assessed using the unpaired *t*-test. ***, $p<0.001$ **C.** IF staining of ORF1p after L1(i) and GL2(i) treatment of PC3 cells. ORF1p signal intensity was measured by quantitative IF at the single cell level, selecting whole cells as the Region of Interest (RoI). Bar, 10 μm. Graphs represent the distribution of ORF1p signal intensities (in arbitrary units) in single cells. A total of 125 GL2(i)- and 190 L1(i)-treated cells were counted in two independent experiments and statistically analyzed using the Mann-Whitney test: ****, $p<0.0001$.

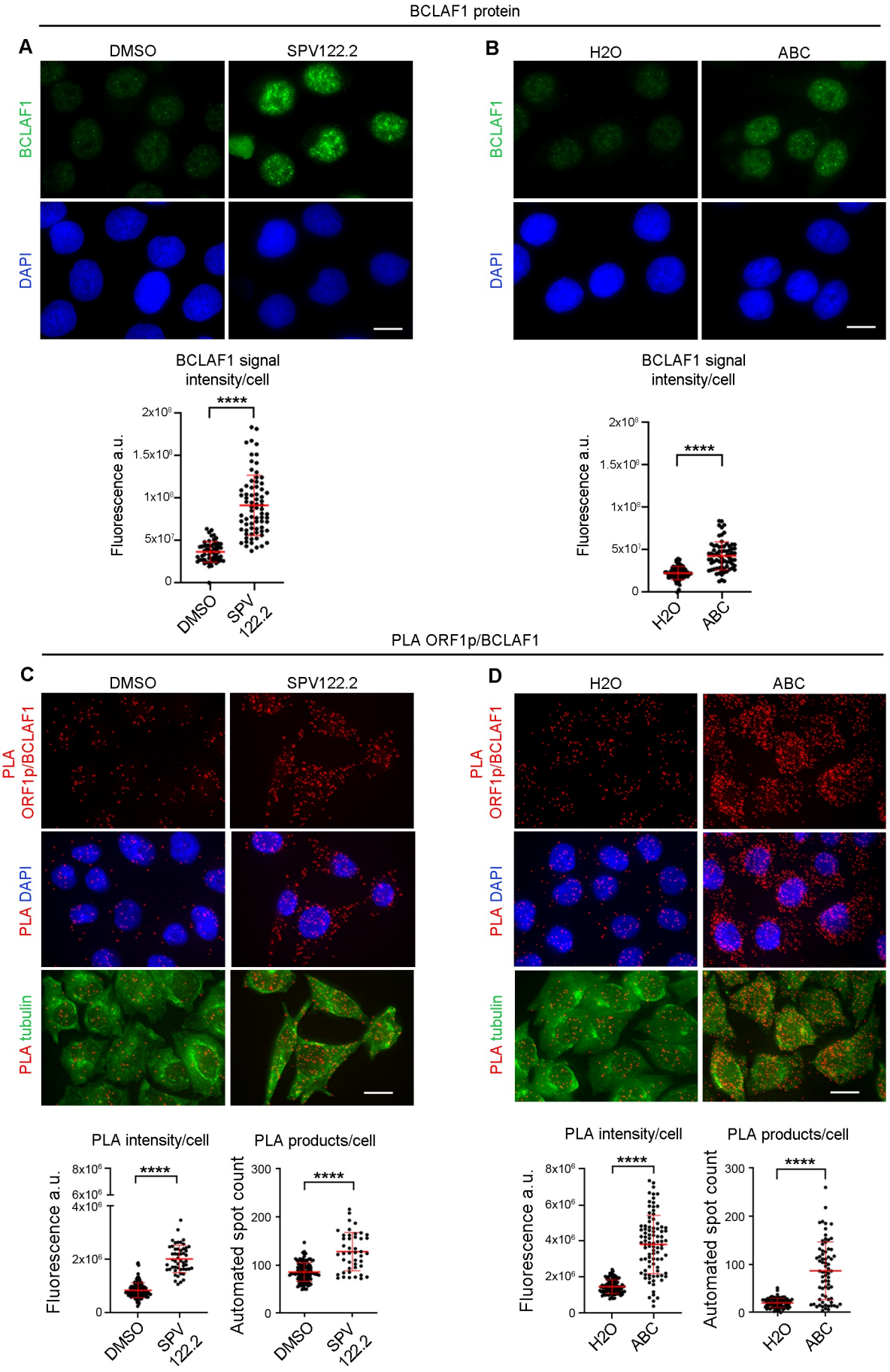

Supplementary Figure 2

Supplementary Fig. 2. **SPV122.2 and ABC up-regulate the DNA damage and stress-responsive factor BCLAF1 and induce the formation of ORF1p/ BCLAF1 ligation products in PC3 cells.** Representative IF fields from PC3 cultures treated with **(A)** SPV122.2 and **(B)** ABC, stained for BCLAF1. BCLAF1 signal intensity was measured on the DAPI mask. Bars, 10 µm. Respective graphs below display the BCLAF1 signal intensity/cell measured in RTI-treated cultures and in their respective controls (DMSO-treated or untreated, H2O). 57 DMSO-, 74 SPV122.2-, 53 H2O-, and 51 ABC-treated cells were analyzed. The presented result was reproduced in a second experiment. In total 75 to 115 cells were analyzed per condition. Statistical analysis was performed using the Mann-Whitney test ****, $p<0.0001$. **C.** PLA assays probing ORF1p and BCLAF1 in DMSO-treated and SPV122.2-treated cultures. **D.** PLA assays probing ORF1p and BCLAF1 in untreated (H2O) and ABC-treated PC3 cultures. The PLA probe is depicted in red. Bars, 10 µm. The graphs quantify the overall PLA fluorescence intensity per cell (# of analyzed cells: DMSO, 120; SPV122.2, 54; H2O, 95; ABC, 92) as well as the number of PLA products per cell ((# of analyzed cells: DMSO, 112; SPV122.2, 55; H2O, 84; ABC, 71) under each condition and demonstrate highly significant increases upon treatment with both RTIs. Data were statistically analyzed using the Mann-Whitney test. ****, $p<0.0001$.

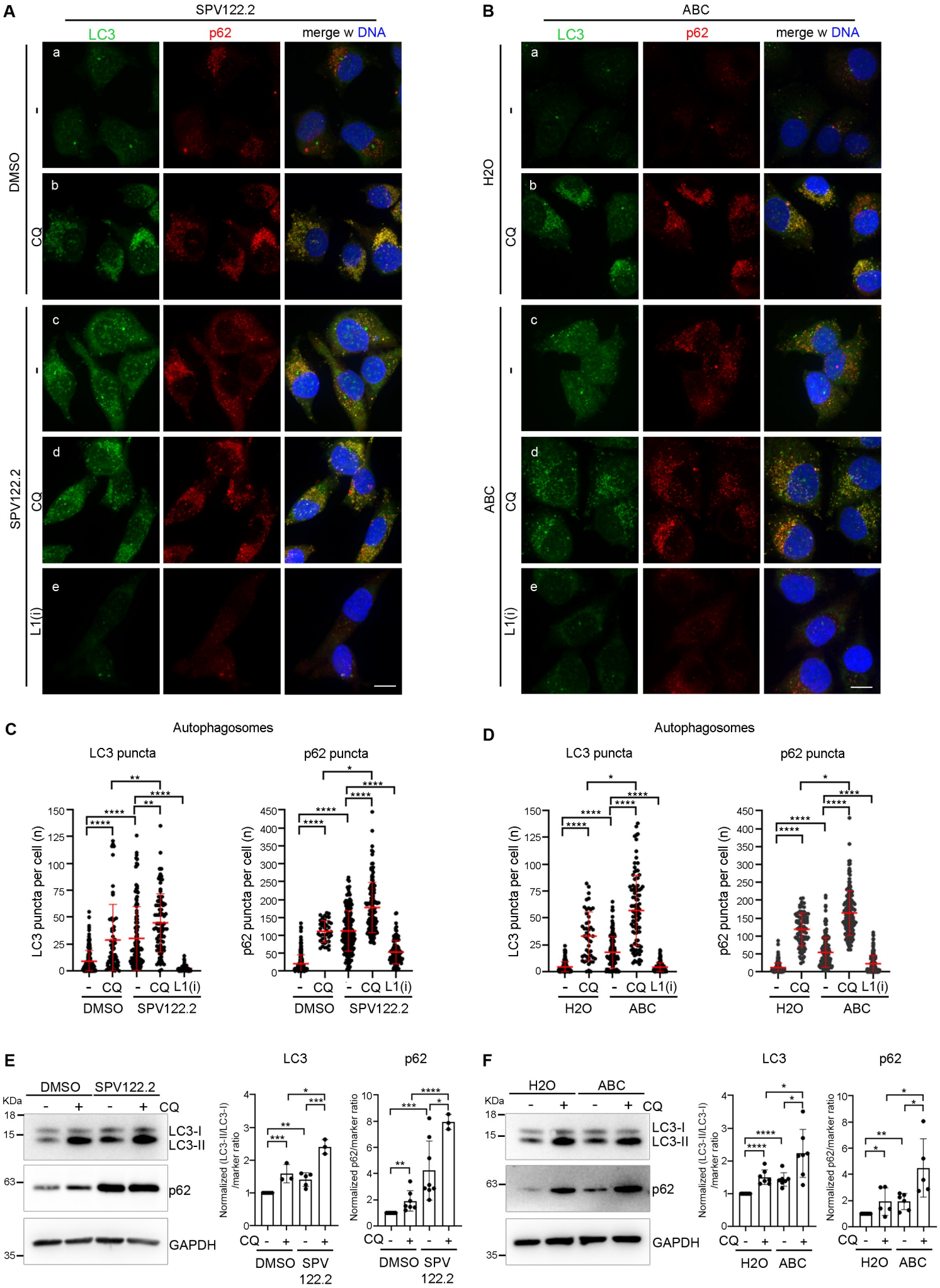

Supplementary Figure 3

Supplementary Fig. 3. SPV122.2 and ABC induce autophagy markers in PC3 cells in a *L1*-dependent manner. A. Single-cell IF staining of the autophagy markers LC3 (green) and p62 (red) in SPV122.2-treated PC3 cultures: upon treatment with SPV122.2 (panel c), both proteins show a significant increase in amount and form cytoplasmic granules (indicated as puncta) compared to DMSO-treated cultures (panel a). The addition of chloroquine (CQ) increased puncta formation in both control cells (panel b) and SPV122.2-treated cultures (panel d); in contrast, L1-specific siRNAs [L1(i)] abolished that increase in response to SPV122.2 (panel e). **B.** Parallel PC3 cultures were subjected to single-cell IF staining of LC3 and p62 proteins upon ABC treatment: both proteins show a highly significant increase in ABC-treated (panel c) compared to untreated control cells (H2O, panel a); that increase is further strengthened upon CQ addition (panels b and d) and is abrogated by transfection of cells with L1(i) siRNAs (panel e). Bars, 10 μm. **C.** Quantification of autophogasomes in PC3 cultures in SPV122.2 assays; # of counted cells (LC3 puncta): DMSO, 170; CQ, 60; SPV122.2, 130; SPV122.2 + CQ, 90; SPV122.2 + L1(i), 70; (p62 puncta): DMSO, 100; CQ, 43; SPV122.2, 180; SPV122.2 + CQ, 140; SPV122.2 + L1(i), 180; **D.** Quantification of autophogasomes in ABC assays; # of analyzed cells (LC3 puncta): H2O, 160; CQ, 50; ABC, 125; ABC + CQ, 100; ABC + L1(i), 135; p62 puncta : H2O, 100; CQ, 100; ABC, 185; ABC + CQ, 160; ABC + L1(i), 200. Two independent experiments were analyzed. The Kruskal-Wallis test (Dunn's multiple comparison test) was used for statistical analysis. ****, $p<0.0001$; **, $p<0.01$; *, $p<0.05$. **E.** Immunoblot analysis of LC3-II/LC3-I forms and of p62 protein in SPV122.2-treated cells vs. DMSO control cultures. GAPDH served as a loading control. Histograms present the ratio of LC3-II (lipidated) to LC3-I forms, and the abundance of p62 protein, normalized to GAPDH. In order to pool data from three independent experiments, values measured in DMSO controls are set as 1. **F.** Immunoblot analysis of LC3-II/LC3-I forms and of p62 protein in ABC-treated cells vs. H2O control cultures. GAPDH served as a loading control. Histograms present the ratio of LC3-II to LC3-I forms, and the abundance of p62 protein, normalized to GAPDH. In order to pool data from three independent experiments, values measured in H2O controls are set as 1. Statistical significance was calculated using the unpaired Student's *t*-test, with ****, $p<0.0001$; ***, $p<0.001$; **, $p<0.01$; *, $p<0.05$.

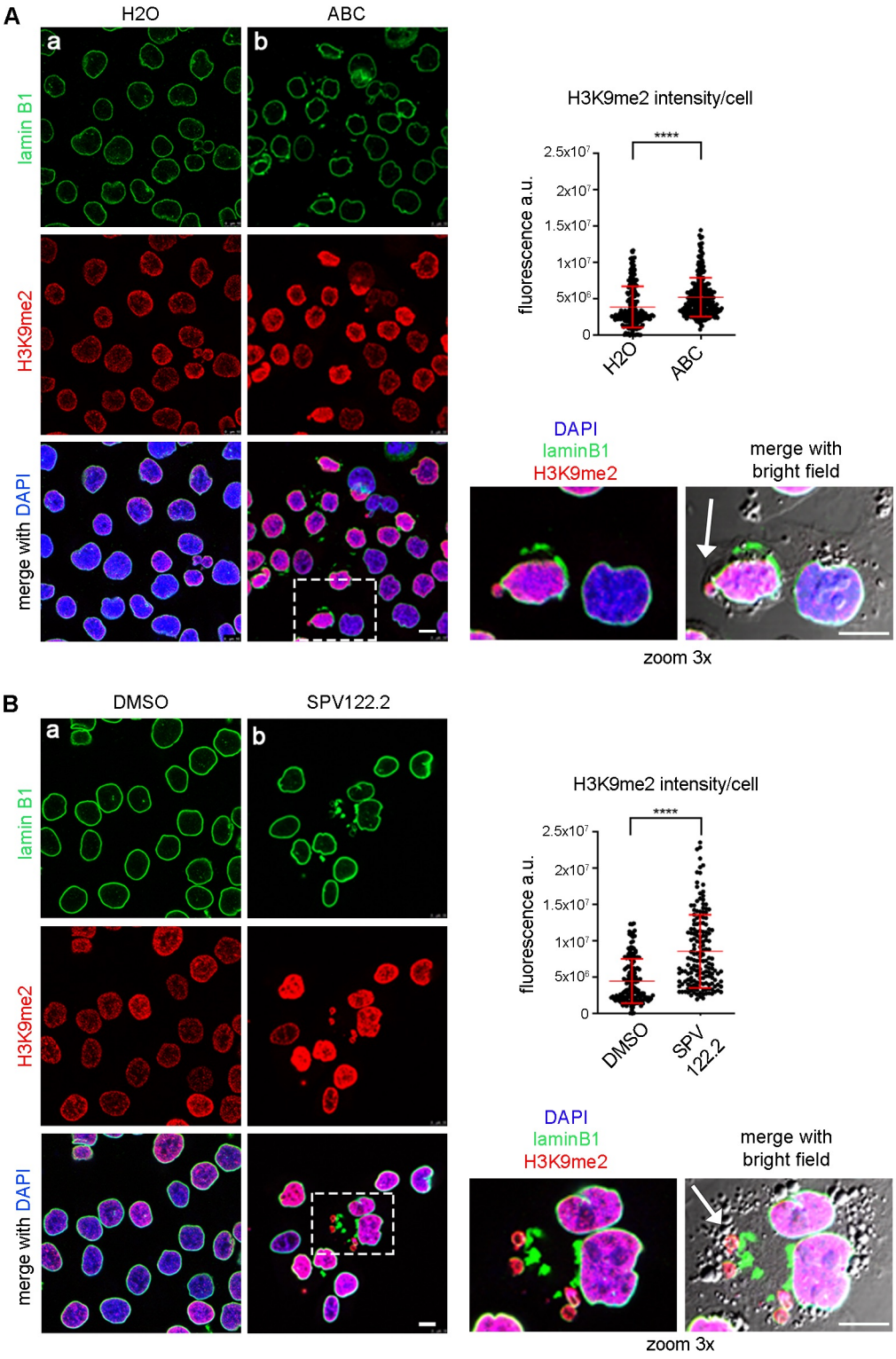

Supplementary Figure 4

Supplementary Fig. 4. **IF analysis of lamin B1 and methylated histone H3 at lysine 9 in PC3 cell treated with SPV122.2 and ABC.**

A. ABC treatment (panel b) induces lamin B1 fragmentation (green), associated with methylated histone H3-containing chromatin (anti-H3K9me2 antibody, red), often expelled from the nucleus, suggestive of micronuclei formation; an example is arrowed in the zoom-in panel. These structures are absent from untreated PC3 control cells (H2O, panel a). **B.** Similar structures (arrowed in the zoom-in panel) are observed in SPV122.2-treated PC3 cultures (panel b), but not in DMSO-treated (panel a) controls. Respective graphs quantify the increase in H3K9me2 induced by RTIs (# of cells analyzed in two independent experiments: H2O, 160; ABC, 170; DMSO, 60; SPV122.2, 75). Statistical significance was calculated using the Mann-Whitney test. ****p<0.0001. **C-D.** DIC microscopy (**C**) and immunofluorescence staining of cytoskeletal tubulin (**D**) indicate that SPV122.2-induced micronuclei are intracellular. Note the invagination of lamin B1 superimposed to the DIC image in (**C**). Bars, 10 μm.

Supplementary Table 1. List of antibodies used in this study

Antibody	Host	Source	Catalog	analysis	Dilution
BCLAF1	rabbit	Thermo Fisher	PA5-55686	IF, PLA	1:500
GAPDH	mouse	Santa Cruz	SC-47724	WB	1:1000
γ-H2AX	rabbit	Cell signaling	9718S	IF, PLA	1:400
H3K9met2	mouse	Millipore	07-411	IF	1:250
Lamin B1	rabbit	Abcam	Ab16048	IF, PLA	1:400
Lamin B1	chicken	Abcam	Ab90169	IF	1:100
LC3B/LC3-II	rabbit	Cell Signaling	2775S	IF	1:250
LC3B/LC3-II	rabbit	Sigma	L7543	WB	1:1000
ORF1p (anti-L1)	mouse	Millipore	MABC1152	IF, PLA, WB	1:50/1:2000
p62/SQSTHM1	mouse	Santa Cruz	SC-28359	IF, WB	1:250/1:200
α-tubulin	mouse	Sigma	T9026	IF, WB	1:1000
β-tubulin	rabbit	Abcam	Ab6046	IF	1:300
β-tubulin	chicken	Abcam	Ab41489	PLA	1:100

Reading keys for Supplementary Data 1. ORF1p IP partner enrichment in Stampidine *vs* control; ORF1p IP partner enrichment in Islatravir *vs* control

Output for ORF1p_IP_Stampidine_Enrichment

Output for ORF1p_IP_Islatravir_Enrichment

Reading keys

Column	Description
uniprotID	Protein Identification from UNIPROTID database
case.avg	Average log LFQ from the treatment with the drug
control.avg	Average log LFQ from the control treatment (DMSO)
logFC	Log Fold Change
Gene.names	Gene names
p_values_adjust	p value adjusted by FDR method after t-test right-tail
Common	Proteins in common between drugs
DNA_Damage_Repair	Proteins related to DNA Damage/Repair (Reactome R-HSA-2559586 and R-HSA-73894)
Splicing	Proteins related to Splicing (Reactome R-HSA-72203)

Raw Western Blots - Fig. 1C

ChemiDoc Imaging system - Biorad

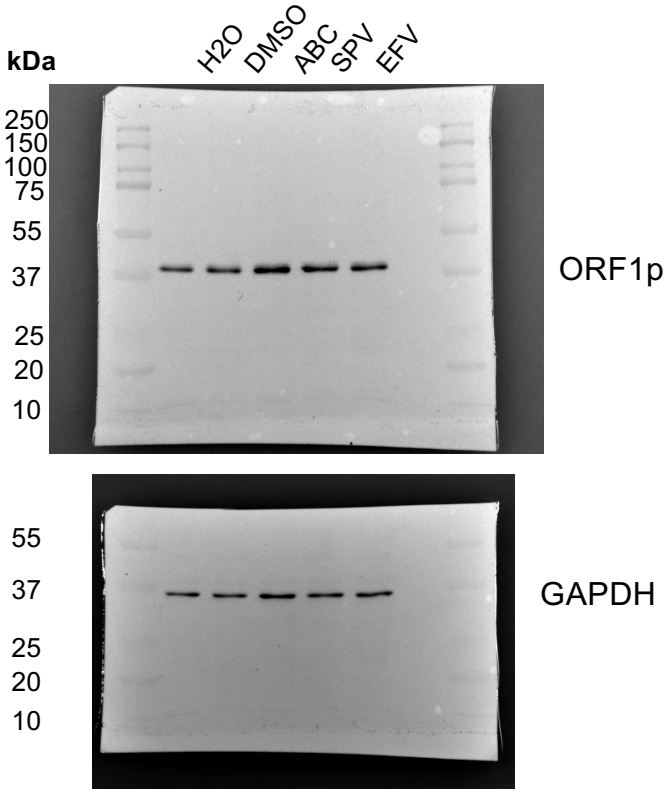

Raw Western Blots - Supplementary Fig. S3E-F

Azure Imaging system – Azure biosystems